Behavioral Study of Alumina Nanoparticles in Pool Boiling Heat Transfer on a Vertical Surface

Ramakrishna N. Hegde,[1] R.P. Reddy,[2] and Srikanth S. Rao[3]
[1]National Institute of Technology, Surathkal, Department of Mechanical Engineering,
M.S. Ramaiah Institute of Technology, M S R Nagar, Bangalore, India
[2]Reva Institute of Technology, Yelahanka, Bangalore, India
[3]Department of Mechanical Engineering, National Institute of Technology, Surathkal, India

Experiments were carried out to investigate the pool boiling of alumina-water nanofluid at 0.1 g/l to 0.5 g/l of distilled water, and the nucleate pool boiling heat transfer of pure water and nanofluid at different mass concentrations were compared at and above the atmospheric pressure. At atmospheric pressure, different concentrations of nanofluids display different degrees of deterioration in boiling heat transfer. The effect of pressure and concentration of nanoparticles revealed significant enhancement in heat flux and deterioration in pool boiling. The heat transfer coefficient of 0.5 g/l alumina-water nanofluid was compared with pure water and clearly indicates deterioration. At all pressures the heat transfer coefficients of the nanofluid were lower than those of pure water. Experimental observation revealed particles coating over the heater surface and subsequent SEM inspection of the heater surface showed nanoparticles coating on the surface forming a porous layer. To substantiate the nanoparticle deposition and its effect on heat flux, investigation was done by measuring the surface roughness of the heater surface before and after the experiment. While SEM images of the heater surface revealed nanoparticle deposition, surface roughness of the heater surface confirmed it. Based on the experimental investigations it can be concluded that an optimum thickness of nanoparticles coating favors an increase in heat flux. Higher surface temperature due to the presence of nanoparticles coating results in the deterioration of boiling heat transfer. © 2011 Wiley Periodicals, Inc. Heat Trans Asian Res, 40(6), 495–512, 2011; Published online 6 July 2011 in Wiley Online Library (wileyonlinelibrary.com/journal/htj). DOI 10.1002/htj.20365

Key words: alumina nanofluid, surface roughness, pool boiling, vertical surface

1. Introduction

With the increasing heat transfer rate of the heat exchange equipment, a conventional process fluid with low thermal conductivity can no longer meet the requirements of high-intensity heat transfer. The low thermal property of the heat transfer fluid is a primary limitation to the development of high compactness and effectiveness of heat exchangers. An effective way of improving the thermal conductivity of fluids is to suspend small solid particles in the fluids [1]. Traditionally, solid particles of micrometer or millimeter magnitudes were mixed in the base liquid. Although the solid additives may improve heat transfer coefficient, practical uses are limited because the micrometer- and/or millimeter-sized particles settle rapidly, clog flow channels, erode pipelines, and cause severe pressure drops. The concept of nanofluids refers to a new kind of heat transport fluids by suspending nanoscaled metallic or nonmetallic particles in base fluids. Some experimental investigations [2–5] have revealed that the nanofluids have remarkably higher thermal conductivities than those of conventional pure fluids and have shown that the nanofluids have great potential for heat transfer enhancement. Nanofluids are more suitable for practical application than the existing techniques for enhancing heat transfer by adding millimeter- and/or micrometer-sized particles in fluids. It incurs little or no penalty in pressure drop because the nanoparticles are so small that the nanofluid behaves like a pure fluid.

Recently, studies have been carried out on the heat transfer coefficient of nanofluids in natural and forced flow [6–13]. Most of studies [6–13] carried out to date are limited to the thermal characterization of nanofluids without phase change (boiling, evaporation, or condensation). Nanoparticles in nanofluids can play a vital role in two-phase heat transfer systems. There is a great need to characterize nanofluids in boiling and condensation heat transfer. Compared with the research efforts in thermal conductivity and forced convective heat transfer, relatively few studies have been carried out on the boiling heat transfer, they are all limited to the pool boiling field [14–18], and there is a lack of consistency in the published results.

Cieslinski and Kaczmarczyk [19] have recently conducted pool boiling experiments to establish the influence of nanofluids concentration as well as tube surface material on heat transfer characteristics at atmospheric pressure. They used a horizontal test surface made of smooth copper and stainless steel tubes having a 10 mm OD and 0.6 mm wall thickness. They selected two nanofluids, containing water-Al_2O_3 and water-Cu nanoparticles with concentrations of 0.01%, 0.1%, and 1% by weight. Their results indicated that, independent of concentration, the nanoparticle material (Al_2O_3 and Cu) has almost no influence on heat transfer coefficient while boiling water-Al_2O_3 or water-Cu nanofluids on a smooth copper tube. While the heater material did not affect the boiling heat transfer in 0.1 wt.% of water-Cu nanofluid, a distinctly higher heat transfer coefficient was recorded for a stainless steel tube than for a copper tube for the same heat flux density, independent of concentration.

Coursey and Kim [20], in their experimental findings using an ethanol-based Al_2O_3 nanoparticle, found that even if the concentration was increased by over two orders of magnitude, no enhancement or degradation of heat transfer was observed during boiling on a glass or gold surface. It was attributed to the high wetting nature of ethanol. For ethanol-Al_2O_3 nanofluids and copper surfaces, the nucleate boiling was improved with increasing nanoparticle concentration.

Liu and Liao [21] examined nanofluids, i.e., a mixture of base fluid (water and alcohol), the nanoparticles (CuO and SiO_2) and the surfactant (SDBS).The nanoparticles suspensions consisted of the base liquid and nanoparticles during pool boiling on the face of a copper bar having a 20 mm diameter. The boiling characteristics of the nanofluids and nanoparticles suspensions were poorer compared with those of the base fluids.

Narayan et al. [22] studied the influence of tube orientation on pool boiling heat transfer of water-Al_2O_3 nanofluids with concentrations of 0.25%, 1%, and 2% by weight, on a smooth tube 33 mm in diameter inclined at 0°, 45°, and 90°. They found that the horizontal orientation gave the maximum heat transfer and the boiling performance deteriorated with an increase in nanoparticle concentration.

Trisaksri and Wongwises [23] tested R141b-TiO_2 nanofluids while boiling on a horizontal copper cylinder 28.5 mm in diameter. They discovered that adding a small amount of nanoparticles did not affect the boiling heat transfer, but addition of TiO_2 nanoparticles at 0.03% and 0.05% by volume resulted in deterioration in boiling heat transfer. Moreover, the boiling heat transfer coefficient decreased with increasing particle volume concentrations, especially at higher heat flux.

Kathiravan et al. [24] investigated boiling of water-Cu and water-Cu-SDS nanofluids on a 300-mm square stainless steel plate. They revealed that copper nanoparticles caused a decrease in boiling heat transfer coefficient with water used as the base liquid. The heat transfer coefficient decreased with an increase in concentration of 0.25%, 0.5%, and 1% by weight of nanoparticles for both water-Cu and water-Cu-SDS nanofluids.

Understanding of heat transfer characteristics of nanofluids is very much in an infant stage. This is the reason why this paper intends to explore more on the effect of alumina nanoparticles presence in distilled water and its subsequent role in heat transfer enhancement mechanism in pool boiling.

Nomenclature

A: surface area, m^2
C_p: specific heat, J/kgK
D: diameter of the heater, m
g: gravitational acceleration, ms^{-2}
h: heat transfer coefficient, W/m^2K
h_{fg}: latent heat of vaporization, Jkg^{-1}
I: current, A
k: thermal conductivity, $Wm^{-1}K^{-1}$
L: length, m
M: molecular weight
P: pressure, Pa
q: heat flux, $Wm^{-2}\ K^{-1}$
T: temperature, K
U: uncertainty
V: voltage, V
w: weight concentration (g/l), wall
W: watt, W

Greek Symbols

ε: rms value of surface roughness
ρ: density, kgm^{-3}
σ: surface tension, Nm^{-1}
μ: viscosity, m^2s^{-1}

Subscripts

c: critical
HF: heat flux
f: fluid
m: mass
max: maximum
nb: nucleate boiling
p: particle
s: surface
L: length
v: vapor

2. Pool Boiling Experiment

The pool boiling experiment was carried out after preparing and characterizing the nanofluid as discussed below.

2.1 Preparation and characterization of nanofluids

The alumina nanoparticles manufactured by NaBond Technologies Corporation Limited were procured to prepare nanofluids; details are given in Table 1 below.

To ensure no agglomeration, any one of the following methods suggested by Xuan and Li [25] viz. changing the pH value of the suspension, using dispersants, or using ultrasonic vibration can be followed. All these methods are aimed at changing the surface properties of suspended particles and subsequently suppressing the formation of particle clusters. In this study, dispersants were not used for stabilization as the addition of dispersants would influence the heat transfer characteristics of nanofluids. The nanofluid was stirred in a high-speed homogenizer for 9 hours. The test fluid sample was collected in a glass vessel and the particle size was confirmed to be in the range of 10 nm to 100 nm with an average of 50 nm as provided by the manufacturer. Figure 1 shows the TEM image of nanoparticles dispersed in distilled water having spherical shapes.

Figure 2 shows the photograph of the test samples at different mass concentrations of alumina nanoparticles with negligible agglomeration even after 9 hrs.

Table 1. Properties of Alumina Nanofluid

Items	Alumina
Content of Alumina	≥ 99%
Average particle size	80 nm
Specific surface area	100 m^2/g

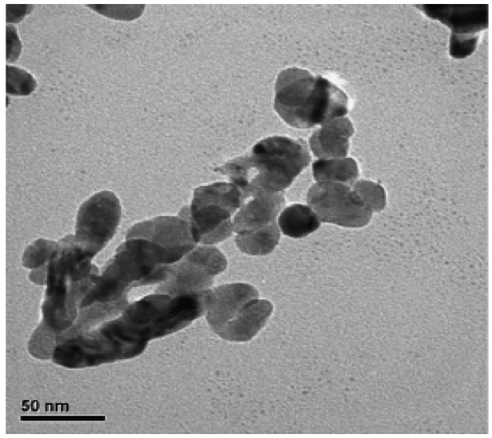

Fig. 1. Characteristics of nanofluid: TEM photograph of alumina nanoparticles.

2.2 Pool boiling experiments

Figure 3 shows the schematic diagram of the experimental setup. It consists of a boiling vessel of 80 mm diameter and 200 mm long made up of SS 316 fitted with flanges at the top and at the bottom with due provisions for liquid charging, condenser cooling water inlet and outlet, vacuum pump, pressure transducer, thermocouples, mounting the test heater section, and drain. The test section is a cylindrical vertical surface of 6 mm diameter and 17 mm long with two thermocouples embedded into the surface 5 mm apart at a depth of 1 mm on the periphery. The test section is heated by an electrical heating element of 1 kW capacity. The heating element is connected to a wattmeter through a dimmer stat to vary the heat input during experimentation.

Two thermocouples placed inside the boiling vessel are used to measure liquid and vapor temperatures. The boiling vessel is well insulated to ensure minimum heat loss to the surroundings. Figure 4 shows the photographic view of the vertical heater surface.

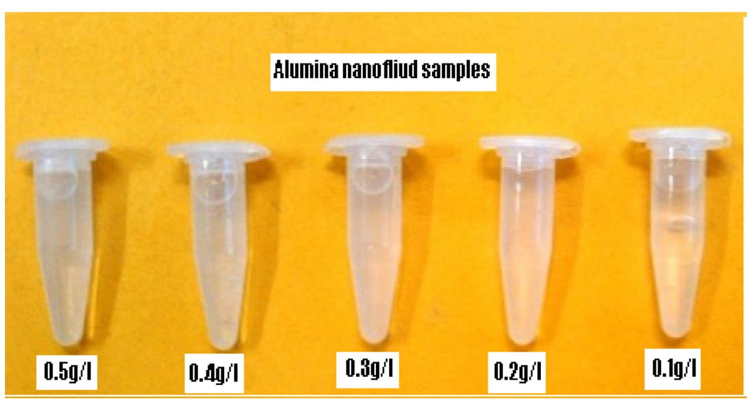

Fig. 2. Test samples at different mass concentrations. [Color figure can be viewed in the online issue, which is available at wileyonlinelibrary.com/journal/htj.]

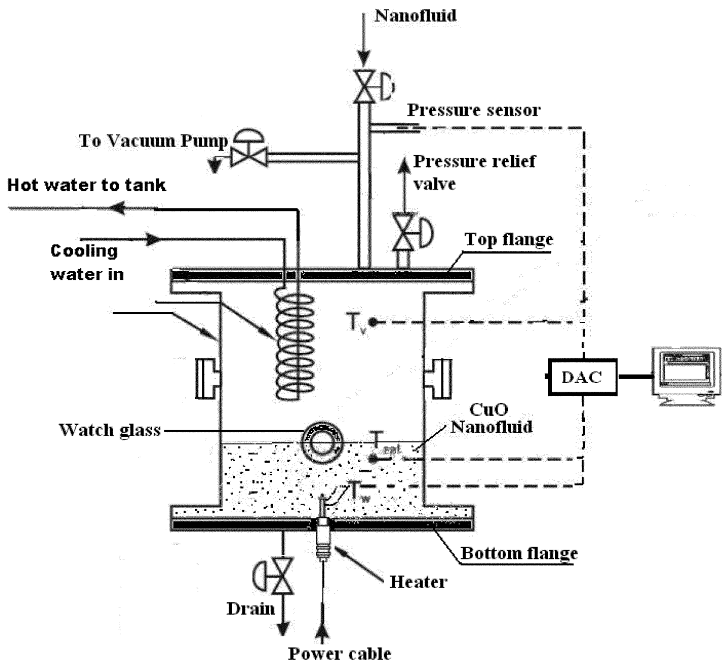

Fig. 3. Schematic diagram of experimental setup.

Since the heating surface is completely immersed in the liquid, most of the heat input is utilized for convective pool boiling with negligible room for conduction loss into the surrounding atmosphere. The detailed cut section of the heater is shown in Fig. 4(b).

Heating surface details:

1, Terminal shell: The outer casing and terminal are zinc coated to resist corrosion.

2, Insulator has exceptional strength, thermal conductivity ensuring no short circuit while the casing provides sufficient heat resistance.

3, Rubber seal: The rubber seal prevents air from seeping through and thereby corroding the coil.

4, Insulation: Electrical insulation of the coil is provided by firmly packing magnesium oxide powder which also acts as an efficient heat conductor.

5. Regulating coil: The main coil acts as a regulator to control and sustain temperature rise and rapid warm up.

6. Coil connection: Laser welding connects the regulating and heating coil to maintain their positions at all times while maintaining constant resistance characteristics.

7. Heating coil: A short tapered section inside the end of the heater ensures quick heating while the tapered tip improves heating efficiency.

Before starting the experiment, the boiling chamber was evacuated using a vacuum pump. The boiling vessel was then filled with alumina-water nanofluid. The experimentation was carried out at atmospheric conditions. Heat input to the test section was given in steps by varying the variac. The set pressure was maintained constant throughout the experiment by using a condenser through which cooling water is circulated. A pressure transducer and a proportional integral derivative (PID)

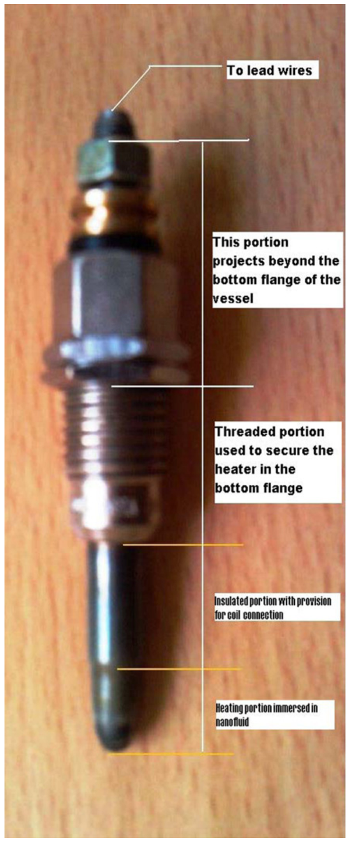

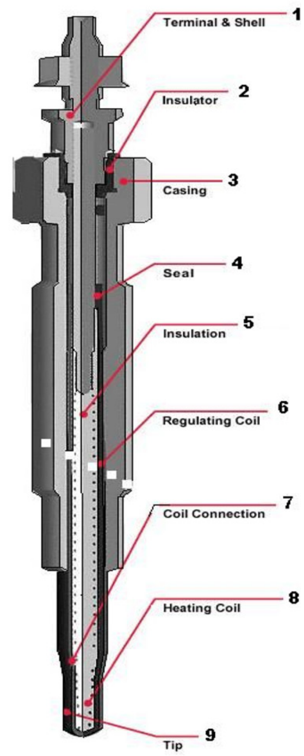

Fig. 4. (a) Photograph of heater; (b) cut section of heater. [Color figure can be viewed in the online issue, which is available at wileyonlinelibrary.com/journal/htj.]

pressure controller are used to sense and maintain the required pressure. The PID senses the pressure level in the boiling chamber through the pressure transducer and compares it with the set value fed to it. After ensuring the steady state conditions, liquid, vapor, heater surface temperatures, system pressure, and heat input were logged in the Data Acquisition System. Care was taken not to reach the critical value of heat flux (input was maintained around 800 W maximum) as this would lead to the "burn out" point, melting the heater itself. The heat flux q is calculated using the following relation.

$$q = \frac{Q}{A} \tag{4}$$

Heat transfer coefficient between the surface and the liquid is calculated by applying Newton's law of cooling

$$h = \frac{q}{T_w - T_s} \tag{5}$$

where T_w is the average of surface temperatures recorded by thermocouples.

2.3 Experimental uncertainty

Major sources of uncertainty are due to measurement in test surface temperature, liquid temperature, system pressure, and heat input. The experimental uncertainty mainly including the parameters like applied heat input in *W*, liquid temperature, and measurement in concentration is calculated using the following relation proposed by Holman [26] as follows.

$$U_{q_{HF}} = q_{HF}\left\{\left(\frac{U_{W\max}}{W_{\max}}\right)^2 + \left(\frac{U_{P\max}}{P_{\max}}\right)^2 + \left(\frac{U_{T_W}}{T_W}\right)^2 + \left(\frac{U_{T_L}}{T_L}\right)^2 + \left(\frac{U_V}{V}\right)^2\right\}^{1/2} \tag{6}$$

The uncertainties of the applied wattage, pressure, surface, and liquid temperatures and concentrations are respectively found to be 1%, 0.7%, and 1% respectively. From the above analysis, the maximum uncertainty for pool boiling heat flux was estimated to be 4.96%.The maximum uncertainty in the wall superheat values is ±1 °C. The maximum uncertainty in the heat transfer coefficient is 7%.

3. Results and Discussion

Based on the experimentation with alumina nanoparticles in distilled water, boiling characteristics of water-based alumina nanofluid with changed concentrations and pressure are discussed below.

3.1 The boiling characteristics of the water-based alumina nanofluid

Figure 5 shows the pool boiling experimental results for water-based alumina nanofluid at different mass concentrations ranging from 0.1 g/l to 0.5 g/l of distilled water under atmospheric pressure. In order to compare the boiling heat transfer among water and nanofluids, the saturated temperature of pure water at 100 °C was taken as the uniform standard for the nanofluids as well.

In order to check the reliability of the apparatus, the experimental results were compared with the data predicted by the well known correlations. Rohsenow [27] proposed the following correlation to determine the heat transfer coefficient, which is quite commonly used by researchers:

$$h_{nb} = \frac{1}{C_{sf}}\left[\frac{C_{pf}\,q}{h_{fg}}\right]\left[\frac{q}{\mu_f h_{fg}}\left(\frac{\sigma_f}{g(\rho_f - \rho_v)}\right)^{\frac{1}{2}}\right]^{-n}\left[\frac{\mu C_p}{k}\right]_f^{-(m+1)} \tag{7}$$

In this calculation, *m* is taken as 0 and C_{sf} as 0.0015 which is the empirical constant of stainless steel and water surface fluid combination.

Cooper [28] proposed a correlation to predict the nucleate pool boiling heat transfer coefficient. In his correlation, the heat transfer coefficient was presented as a function of the heat flux, reduced pressure, molecular weight of the liquid, and the surface roughness. For boiling on horizontal plane surfaces,

$$h_{nb} = 55(p_r)^{0.12-0.4343\ln R_p}(-0.4343\ln p_r)^{-0.55}M^{-0.5}q^{0.67} \tag{8}$$

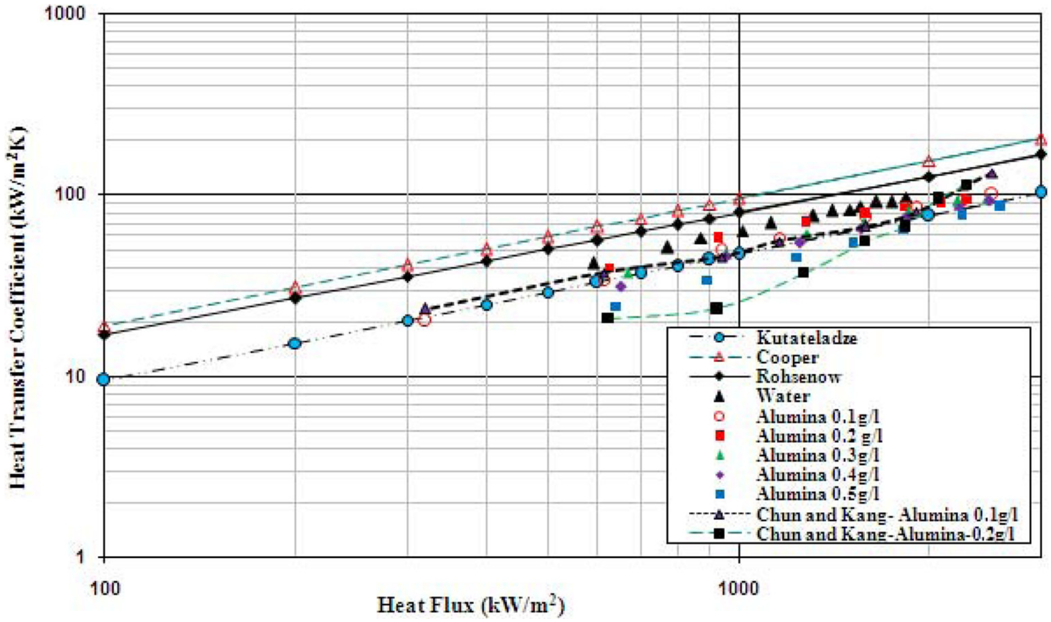

Fig. 5. Comparison of experimental data with popular correlations. [Color figure can be viewed in the online issue, which is available at wileyonlinelibrary.com/journal/htj.]

An increase in surface roughness has the effect of increasing the nucleate boiling heat transfer coefficient. Surface roughness may be affected by fouling, corrosion, and oxidation of the surface. When surface roughness is unknown, it is set to 1.0 μm.

Kutateladze [29] has proposed the following correlation which predicts pool boiling in terms of Nusselt and Prandtl numbers.

$$\frac{h_{nb}d}{k} = 0.44\left[\left(\frac{10^{-4}qP}{gh_{fg}\rho_v}\right)\left(\frac{\rho_f}{\rho_f-\rho_v}\right)\right]^{0.7}\mathrm{Pr}^{0.35} \tag{9}$$

Chun and Kang [30] empirically investigated the effect of surface roughness on pool boiling outside tubes. They also suggested two empirical correlations: one for horizontal tubes and the other for vertical tubes which contain the effect of surface roughness as a parameter. They proposed the following relation for heat transfer coefficient for stainless steel tubes (D = 9.7 – 25.4 mm) in water for a vertical orientation.

$$h_{nb} = 0.024\varepsilon^{0.672}\frac{\Delta T^{3.862}}{D^{1.656}} \tag{10}$$

From the figure it can be observed that the boiling heat transfer coefficient of water agrees reasonably well with Eq. (7) having a deviation of 6.5% even at a higher value of heat flux. At lower concentrations (0.1 g/l) Eq. (10) matches well with the experimental data but deviates at higher concentrations which can be attributed to the smaller diameter of the test surface.

Comparison between experimental data using nanofluids and the Rohsenow correlation show that the correlation has great potential to predict the pool boiling behavior with an appropriate modified liquid-surface combination ($C_{sf} = 0.030$) and change physical properties of the base fluid as shown in Fig. 6.

3.2 Effect of nanofluid concentration

The experiments were carried out to investigate the pool boiling of alumina-water nanofluid in distilled water at 0.1 g/l to 0.5 g/l of distilled water and the nucleate pool boiling heat transfer of pure water and nanofluid at different mass concentrations were compared. As shown in Fig. 7 at atmospheric pressure, different concentrations of nanofluids display different degrees of deterioration in boiling heat transfer. At 0.1 g/l and 0.2 g/l of concentration even though the degree of superheat remains more or less the same, the heat flux increases drastically when compared with water. This indicates that even adding an extremely small amount of nanoparticles can affect the boiling heat transfer to a greater extent. Further addition of alumina nanoparticles (0.3 g/l to 0.5 g/l) results in shifting of the boiling curve to the right, indicating a deterioration of boiling heat transfer. Figure 7 shows clear distinctions between the natural convection stage and nucleate boiling stage. In the case of nanofluids, the natural convection stage continues relatively longer and nucleate boiling is delayed or a higher degree of superheat of the boiling surface is needed for boiling. This is because the range of the excess temperature in the natural convection regime of the nanofluid is wider than that of pure water.

As shown in Fig. 8, at the same heat flux, the heat transfer coefficient at higher concentrations of nanofluid is lower than that at lower concentrations across the range of heat flux. At higher heat flux, the effect of concentration is prominent. Further, it can be observed that for a particular

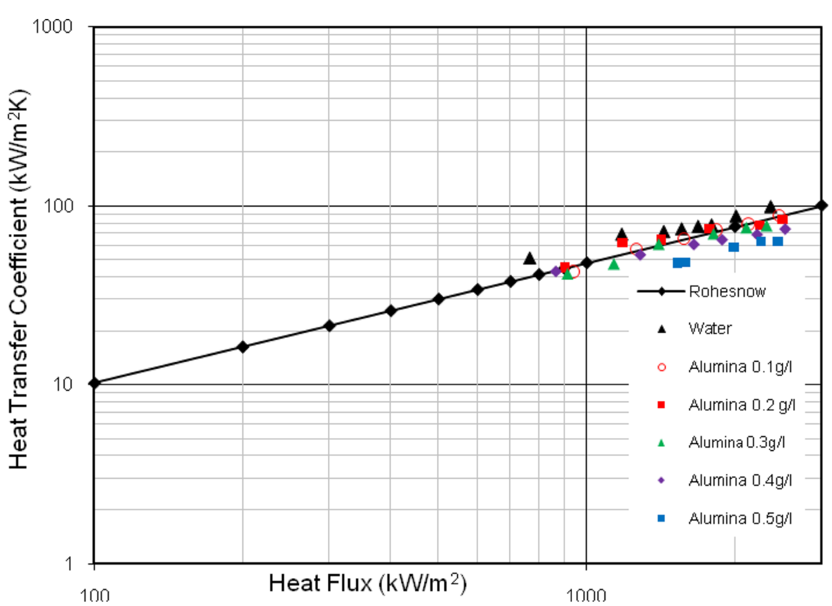

Fig. 6. Comparison of experimental data with modified Rohsenow correlation. [Color figure can be viewed in the online issue, which is available at wileyonlinelibrary.com/journal/htj.]

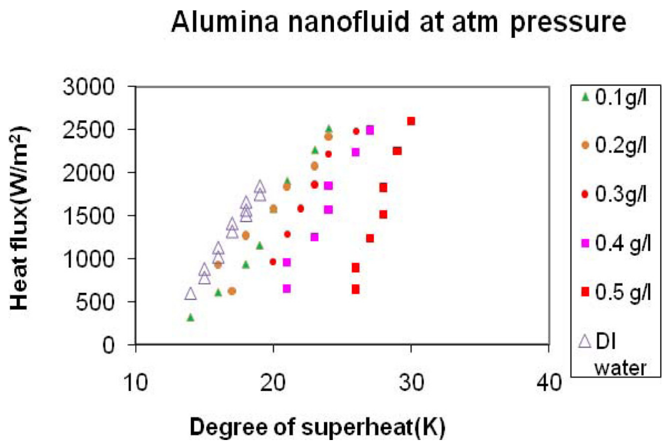

Fig. 7. Boiling curve for five different volume concentrations of alumina nanofluid. [Color figure can be viewed in the online issue, which is available at wileyonlinelibrary.com/journal/htj.]

concentration of nanofluid (0.2 g/l at a heat flux of 2000 kW/m^2) the heat flux is the highest and reduces with higher concentrations. Out of many reasons one possible reason may be the deposition of nanoparticles over the heating surface, the effect of which is discussed in a later section.

3.3 Effect of pressure

Figure 9 shows the relation between heat flux and excess temperature for distilled water and 0.5 g/l of alumina nanofluid at 5 bar. The boiling curve of the working fluid at each pressure appears the same. As the concentration is increased, it is clear that the curve shifts to a higher value of excess temperature due to higher surface temperature.

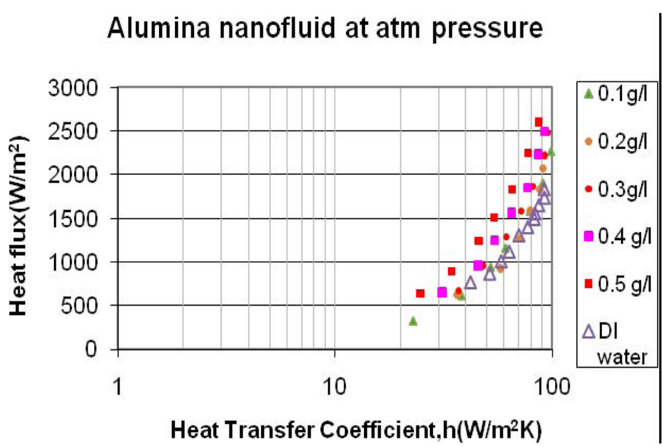

Fig. 8. Heat flux versus heat transfer coefficient. [Color figure can be viewed in the online issue, which is available at wileyonlinelibrary.com/journal/htj.]

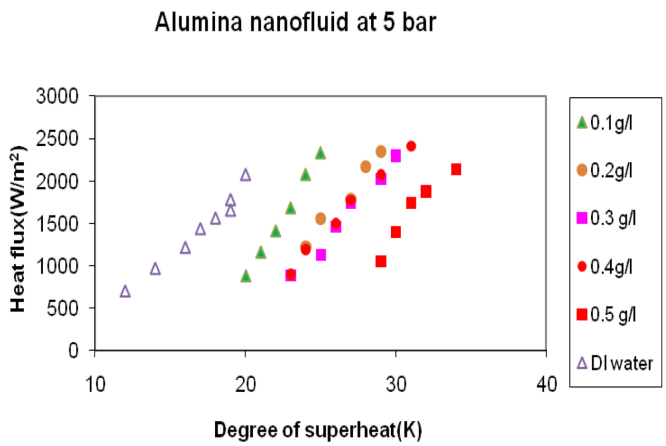

Fig. 9. Boiling curve for 0.5 g/l concentration of alumina nanofluid. [Color figure can be viewed in the online issue, which is available at wileyonlinelibrary.com/journal/htj.]

As shown in Fig. 9, for 0.5 g/l particle concentration at a given higher heat flux, the excess temperature of the alumina-water nanofluid are higher than that of pure water for the entire range of measured data. This shows that, at the same heat flux, nanofluid boiled at a higher surface temperature than the pure water.

The heat transfer coefficient of 0.5 g/l alumina-water nanofluid was compared with pure water and clearly indicates deterioration. At all pressures the heat transfer coefficients of nanofluid were lower than those of pure water. As mentioned above, for pure water the heat transfer coefficient increases with increasing heat flux and pressure. However, for 0.5 g/l alumina-water nanofluid, the increase in heat transfer is significantly less.

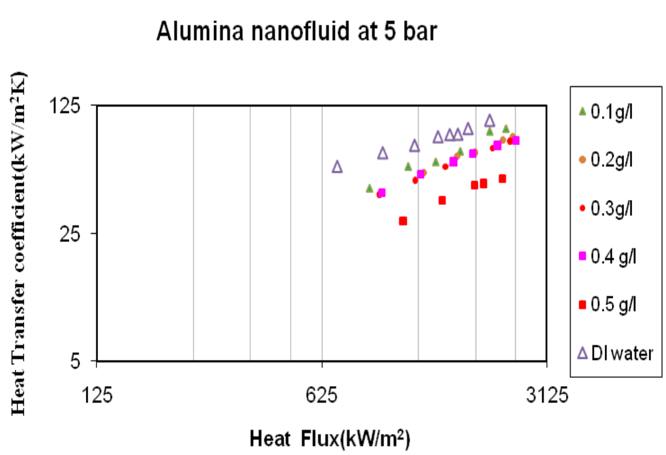

Fig. 10. Heat transfer coefficient versus heat flux. [Color figure can be viewed in the online issue, which is available at wileyonlinelibrary.com/journal/htj.]

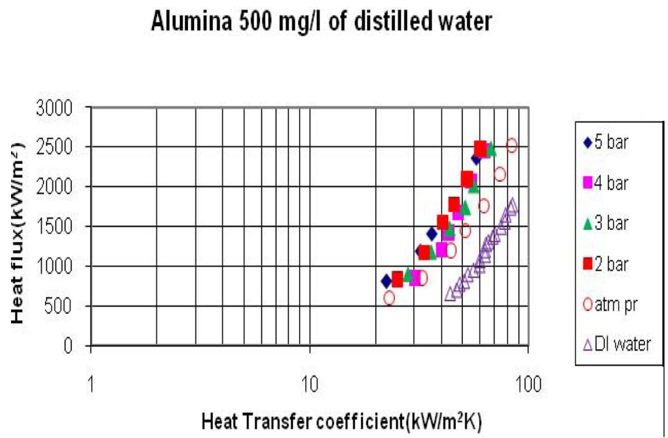

Fig. 11. Heat flux versus heat transfer coefficient at different pressures for a fixed mass concentration of alumina nanofluid. [Color figure can be viewed in the online issue, which is available at wileyonlinelibrary.com/journal/htj.]

Effect of different pressures with a fixed mass concentration of alumina nanofluid is shown in Fig. 11. It can be observed that the heat flux for a given heat transfer coefficient at various pressures are closer together than those of pure water. The presence of 0.5 g/l nanofluid nanoparticles decreases the influence of pressure on the nucleate pool boiling heat transfer especially at high pressure. Also it is evident from Fig. 11 that heat transfer coefficients at specific excess temperature are almost the same at 4 bar and 5 bar.

Figure 12 makes a comparison of heat transfer behavior at atmosphere and 5 bar pressures with different mass concentration of alumina nanofluid. Referring to Fig. 12(a), for a given heat flux the degree of superheat increases with an increase in pressure and is seen by a rightward shift of the

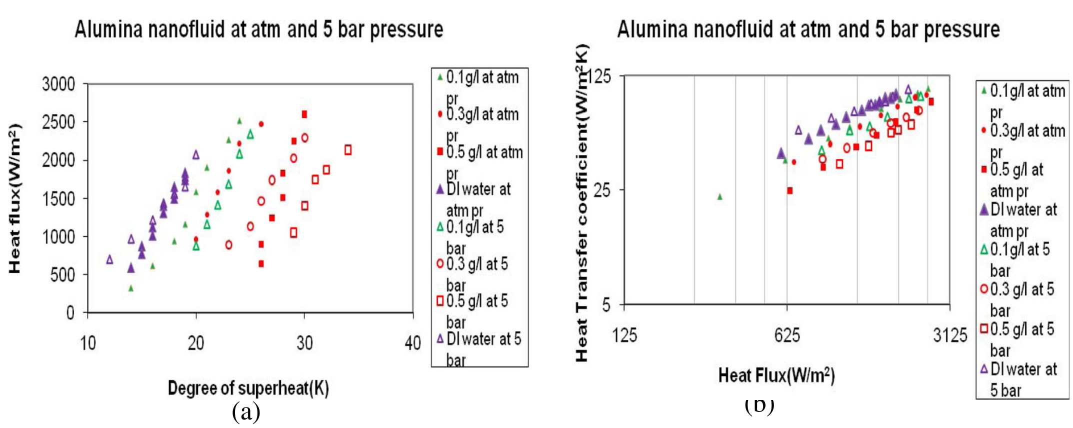

Fig. 12. A comparison of heat transfer behavior at atmosphere and 5 bar pressures with different mass concentrations of alumina nanofluid. [Color figure can be viewed in the online issue, which is available at wileyonlinelibrary.com/journal/htj.]

Table 2. Error Estimation of Predictive Model

Alumina in DI water(g/l)	C	n	Mean error(%)	RMS error(%)
0.1-0.5	0.113	0.73	11.5677	4.43

curve. This reversal trend can be attributed as observed during experimentation to the higher surface temperature due to nanoparticle presence. The effect of pressure on the heat transfer coefficient can be clearly seen in Fig. 12(b) at higher values of heat flux and pressure. The heat transfer coefficient is much higher for a higher heat flux than for a lower value. Further, at very low heat flux there is almost no effect of pressure on the heat transfer coefficient. At a given pressure the variation may be described by the relationship, $h = Cq^n$, where C is a constant which includes the effect of pressure and surface characteristics of the heater. The value of C and n was separately calculated for each concentration using the experimental data (number of data points = 431) and the average value of C and n was taken to predict the final correlation as shown in Table 2.

Figure 13 shows the plot of experimental and predicted values of the heat transfer coefficient based on data points for different mass concentrations of alumina nanofluid at pressures ranging from 1 bar to 5 bars. The predicted equation agrees well within a range of +10 to –10%.

3.4 Changed boiling heat transfer performance

From the above results it is evident that the inclusion of small amounts of nanoparticles tends to change the pool boiling behavior resulting in higher heat flux. In addition there is deterioration of the heat transfer coefficient when compared with pure water. This unexpected heat transfer performance of nanofluids is opposite to their properties as a fluid. Therefore, the reasons for this conflicting performance may be related to differences in the surface characteristics between the boiling surface

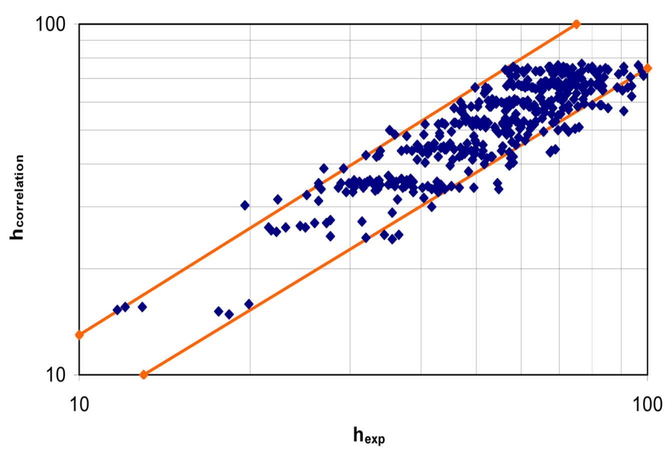

Fig. 13. Experimental and predicted values of heat transfer coefficient. [Color figure can be viewed in the online issue, which is available at wileyonlinelibrary.com/journal/htj.]

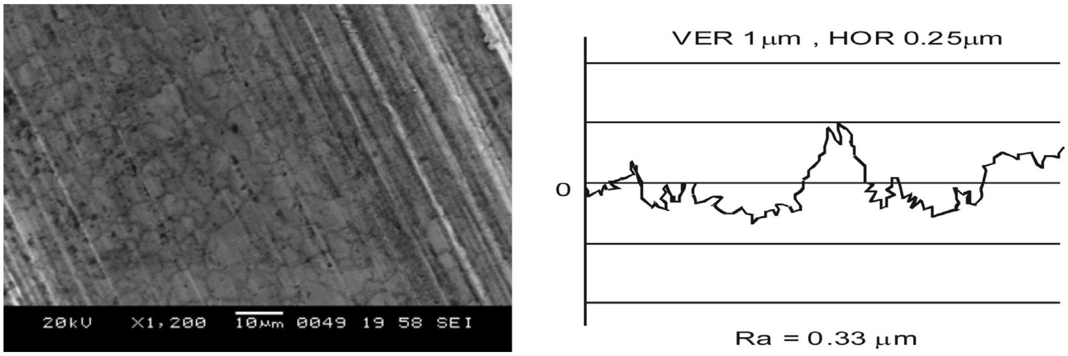

Fig. 14. SEM image of bare heating surface and its surface roughness.

and nanofluids. Hegde et al. [31] found that the surface roughness of the surface considerably decreased changing the boiling characteristics. The measurement results of the present work show that the surface roughness values of test heaters submerged in nanofluids are also decreased on average with increasing particle concentration, as shown in Fig. 14.

The decrease in surface roughness could be due to the deposition of nanoparticles into the microcavities of the porous layer built up as shown in Figs. 15 and 16. High concentration means that the nanofluid contains more nanoparticles that move around themselves or the heated surface, such as the stochastic (Brownian) motion of the particles [32] attaching to the heated surface, which is considered as a kind of fouling as confirmed in the SEM image shown in Fig. 15.

As far as the reason for the increase in heat flux is concerned, it can be attributed to the nanoparticles deposition over the heater surface resulting in higher surface temperature due to higher thermal conductivity of nanoparticles. This increasing trend in heat flux would continue until a particular thickness of coating beyond which a reversal occurs. This means there is an optimum

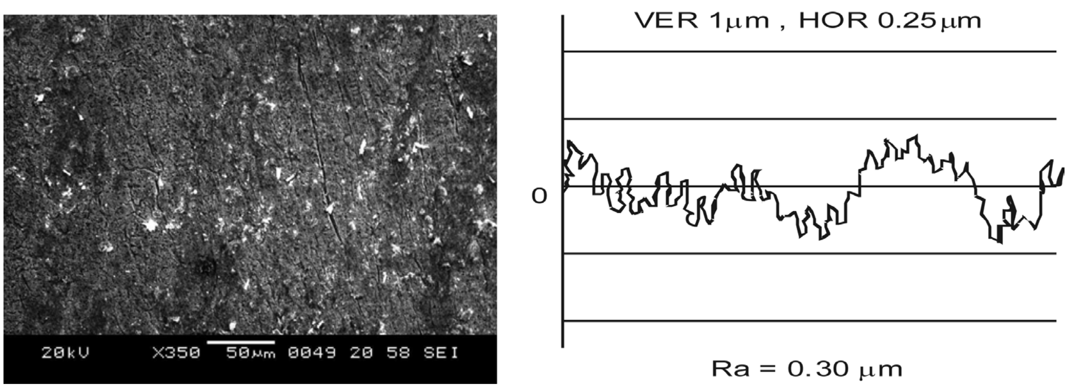

Fig. 15. SEM image showing nanoparticles deposition (0.2 g/l) on the heating surface and surface roughness.

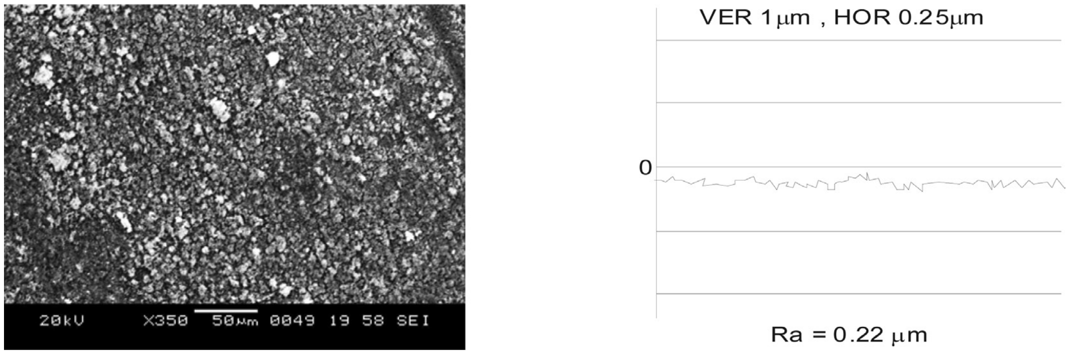

Fig. 16. SEM image showing nanoparticle deposition (0.5 g/l) on the heating surface and surface roughness.

thickness of coating which results in increased heat flux and any addition of coating beyond this will result in a drop in heat flux. Further investigation in this regard is very much solicited.

4. Conclusions

Experimental investigations of pool boiling heat transfer of alumina nanofluids on a vertical heating surface with five mass concentrations ranging from 0.1 g/l to 0.5 g/l of distilled water was done, leading to the following conclusions.

- The surface roughness measurement and the corresponding SEM images of the heater surface, taken for different mass concentrations of nanofluids before and after pool boiling tests, confirmed that the heat flux enhancement of nanofluids was closely related to the surface microstructure and enhanced topography resulting from the deposition of nanoparticles.

- The study also revealed that change in surface roughness not only results from a change in concentration but also leads to decreased surface roughness. The decrease in surface roughness could be due to the deposition of nanoparticles into the microcavities of the porous layer built up due to the stochastic (Brownian) motion of the particles.

- Addition of alumina nanoparticles results in shifting of the boiling curve to the right, indicating deterioration of boiling heat transfer. In the case of nanofluids, the natural convection stage continues relatively longer and nucleate boiling is delayed or a higher degree of superheat of the boiling surface is needed for boiling. The deterioration in nucleate boiling was due to increased particle coating beyond an optimum thickness, thereby inhibiting heat transfer from the test surface.

- Effect of pressure seems to have played no role in the pool boiling behavior of nanofluids. But increased pressure resulted in a rightward shift of the pool boiling curve with nanoparticles as against the behavior of pure water. The reason could be higher surface temperature due to the coating of nanoparticles. However, further investigations are needed in this regard.

Literature Cited

1. Webb RL. Principles of enhanced heat transfer. John Wiley: 1993.
2. Wang X, Xu X, Choi SUS. Thermal conductivity of nanoparticle-fluid mixture. J Thermophys Heat Transf 1999;13:474–480.
3. Lee S, Choi SUS, Li S et al. Measuring thermal conductivity of fluids containing oxide nanoparticles. J Heat Transf 1999;121:280–289.
4. Li Q, Xuan Y. Experimental investigation on transport properties of nanofluids. Heat Transf Sci Technol 2000 (ed. Wang Buxuan), Beijing: Higher Education Press; 2000. p 757–762.
5. Xuan Y, Li Q. Heat transfer enhancement of nanofluids. Int J Heat Fluid Flow 2000;21:58–64.
6. Lee S, Choi SUS. Application of metallic nanoparticle suspensions in advanced cooling systems. In: Proc Int Mech Eng Congress Exhibition Atlanta, USA 1996.
7. Pak KB, Cho YI. Hydrodynamic and heat transfer study of dispersed fluids with submicron metallic oxide particles. Exp Heat Transf 1999;11:151–170.
8. Xuan YM, Li Q. Heat transfer enhancement of nanofluid. Int J Heat Fluid Flow 2000;21:58–64.
9. Xuan YM, Li Q. Investigation on convective heat transfer and flow features of nanofluid. ASME J Heat Transf 2003;125:151–155.
10. Wen DS, Ding YL. Experimental investigation into convective heat transfer of nanofluid at entrance area under laminar flow region. Int J Heat Mass Transf 2004;47:5181–5188.
11. Roy G, Nguyen W, Das SK. Numerical investigation of laminar flow and heat transfer in a radial flow cooling system with the use of nanofluid. Super Lattices Microstruct 2003;35:497–511.
12. Maiga SEB, Nguyen CT, Galanis N, Roy G. Heat transfer behaviors of nanofluid in a uniformly heated tube. Perlattices-Microstruct 2004;26:543–557.
13. Yang Y, Zhang Z, Grulke E, Anderson W, Wu G. Heat transfer properties of nanoparticle-in-fluid dispersions (nanofluid) in laminar flow. Int J Heat Mass Transf 2005;48:1107–1116.
14. Das SK, Putra N, Roetzel W. Pool boiling characteristics of nanofluid. Int J Heat Mass Transf 2003;46:851–862.
15. Vassallo P, Kuman R, Amico SD. Pool boiling heat transfer experiments in silica–water nano-fluids. Int J Heat Mass Transf 2004;47:407–411.
16. Bang IC, Chang SH. Boiling heat transfer performance and phenomena of Al_2O_3–water nanofluid from a plain surface in a pool. Int J Heat Mass Transf 2005;48:2407–2419.
17. Wen DS, Ding YL. Experimental investigation into the pool boiling heat transfer of aqueous based alumina nanofluid. J Nanoparticles Res 2005;7:265–275.
18. You SM, Kim JH, Kim KH. Effect of nanoparticles on critical heat flux of water in pool boiling heat transfer. Appl Phys Lett 2003;83:3374–3376.
19. Cieslinski JT, Kaczmarczyk TZ. Pool boiling of water-Al_2O_3 and water-Cu nanofluids on horizontal smooth tubes. Nanoscale Rese Lett 2010;6:220.
20. Coursey JS, Kim J. Nanofluid boiling: the effect of surface wettability. Int J Heat Fluid Flow 2008;29:1577–1585.
21. Liu Z, Liao L. Sorption and agglutination phenomenon of nanofluids on a plain heating surface during pool boiling. Int J Heat Mass Transf 2005;48:2407–2419.
22. Narayan GP, Anoop KB, Sateesh G, Das SK. Effect of surface orientation on pool boiling heat transfer of nanoparticle suspensions. Int J Multiphase Flow 2008;34:145–160.
23. Trisaksri V, Wongwises S. Nucleate pool boiling heat transfer of TiO2-R141b nanofluids. Int J Heat Mass Transf 2009;52:1582–1588.
24. Kathiravan R, Kumar R, Gupta A, Chandra R. Preparation and pool boiling characteristics of copper nanofluids over a flat plate heater. Int J Heat Mass Transf 2010;53:1673–1681.
25. Xuan Y, Li Q. Heat transfer enhancement of nanofluids. Int J Heat Fluid Flow 2000;21:58–64.

26. Holman JP. Experimental methods for engineers, 7th ed. McGraw-Hill; 2007.
27. Rohsenow WM. A method of correlating heat transfer data for surface boiling of liquids. Trans ASME 1952;74:969–976.
28. Cooper MG. Saturation nucleate pool boiling be a simple correlation. IChemE Symp Ser 1984;86:786–793.
29. Kutateladze SS, Borishansky VM. A concise encyclopedia of heat transfer. Pergamon Press; 1966. Chapter 12.
30. Chun MH, Kang MG. Effects of heat exchanger tube parameters on nucleate pool boiling heat transfer. ASME J Heat Transf 1998;120:468–476.
31. Hegde R, Rao SS, Reddy RP. Critical heat flux enhancement in pool boiling using alumina nanofluids. Heat Transf Asian Res 2010;39:323–331.
32. Jang SP, Stephen U, Choi S. Role of Brownian motion in the enhanced thermal conductivity of nanofluids. Appl Phys Lett 2004;84:4316.

□♦ ♦ ♦□